Journal of Alloys and Compounds 507 (2010) 1–5

Contents lists available at ScienceDirect

Journal of Alloys and Compounds

journal homepage: www.elsevier.com/locate/jallcom

Optimization of thermoelectric properties of type-VIII clathrate $Ba_8Ga_{16}Sn_{30}$ by carrier tuning

Y. Saiga [a,*], K. Suekuni [a], S.K. Deng [a], T. Yamamoto [a], Y. Kono [b], N. Ohya [b], T. Takabatake [a,c]

[a] Department of Quantum Matter, ADSM, Hiroshima University, Higashi-Hiroshima 739-8530, Japan
[b] DENSO CORRORATION Research Laboratories, Nisshin 470-0111, Japan
[c] Institute for Advanced Materials Research, Hiroshima University, Higashi-Hiroshima 739-8530, Japan

ARTICLE INFO

Article history:
Received 11 June 2010
Received in revised form 13 July 2010
Accepted 16 July 2010
Available online 23 July 2010

Keywords:
Type-VIII clathrate
Thermoelectric properties
Thermoelectric figure of merit *ZT*
Carrier tuning

ABSTRACT

Single crystals of type-VIII clathrate $Ba_8Ga_{16}Sn_{30}$ (BGS) with p- and n-type carriers were grown from Ga flux and Sn flux, respectively. With the increase of the initial flux amount, both the electrical resistivity ρ and the absolute value of the Seebeck coefficient $|\alpha|$ are decreased, indicative of effective carrier doping. In the optimally doped samples, the dimensionless thermoelectric figure of merit *ZT* has the maximum values of 1.0 and 0.9 at 450 K for p-and n-type samples, respectively. In aiming at further increase of the *ZT* value, Sb was substituted for Sn in BGS. It is found that the Ga content in the crystals unexpectedly increases with the increase of Sb content and thus the crystal composition is described as $Ba_8Ga_{16+x}Sn_{30-x-y}Sb_y$ ($x < 0.9$, $y < 0.9$). The *ZT* value for the p-type sample with $x = y = 0.7$ has the maximum of 1.0 at around 480 K.

1. Introduction

Most waste heat from factories such as cement production, glass manufacture, and aluminum smelting has the temperature below 700 K. To convert such industrial waste heat to electricity, various types of thermoelectric materials have been so far synthesized [1,2]. For a given material, the dimensionless thermoelectric figure of merit *ZT* is defined as $ZT = \alpha^2 T/\rho\kappa$, where α, ρ, and κ are the Seebeck coefficient, electrical resistivity, and thermal conductivity, respectively. There are a few materials such as $AgPb_{18}TeSb_{20}$ and Zn_4Sb_3 with *ZT* values above 1.0 in the temperature range between 500 K and 600 K [3,4]. However, $AgPb_{18}TeSb_{20}$ contains rare and toxic elements Te and Pb, and Zn_4Sb_3 is degraded easily by thermal hysteresis. To apply the material into practice in the temperature range between 500 K and 600 K, developments of non-toxic and stable materials are urgently needed.

Intermetallic clathrates consist of three-dimensional frameworks of cages where guest atoms can reside. The structural properties as well as the potential as thermoelectrics have been reported in review articles [5–8]. In type-I clathrates $Ba_8Ga_{16}X_{30}$ (X = Si, Ge, and Sn), for example, the composition is valence balanced as each of 8 Ba donates two electrons and each of 16 Ga utilizes one of the two electrons for bonding within the framework [8]. Therefore, it is expected that these clathrates behave as semiconductor and small deviation from the ideal stoichiometry causes charge carriers in real materials. In the case of $Ba_8Ga_{16}Ge_{30}$, excess Ga or Ge results in the composition $Ba_8Ga_{16-x}Ge_{30+x}$ with p-type ($x < 0$) or n-type ($x > 0$) carriers, respectively. In these samples, $|\alpha|$ exceeds 100 μV/K and κ is below 2 W/mK at room temperature. The optimally doped n-type sample with $x = 0.25$ has the maximum $ZT = 0.86$ at 950 K [9,10]. Similarly, $Ba_8Ga_{16}Si_{30}$ and $Sr_8Ga_{16}Ge_{30}$ exhibit *ZT* values 0.9 at 870 K and 0.6 at 800 K, respectively [11,12]. These compounds were regarded as examples those fulfill the phonon glass and electron crystal concept proposed by Slack [13].

$Ba_8Ga_{16}Sn_{30}$ (BGS) has two modifications of type-I and type-VIII, both of which are composed of 46 cage atoms of Ga/Sn and 8 guest atoms of Ba [14,15]. For the type-I, the Ba atoms are encapsulated in two kind of cages; tetrakaidecahedra and dodecahedra, while for the type-VIII the Ba atoms are in one kind of cage; distorted dodecahedra [16]. Type-I BGS shows glass-like thermal conductivity whose value is smaller than that of amorphous silica [17,18]. For type-I BGS single crystals, the room temperature *ZT* value is no more than 0.3 due to the high electrical resistivity exceeding 10 mΩ cm in spite of the very small κ of 0.4 W/mK. Both Ga flux and Sn flux have been used for the growth of type-VIII BGS single crystals whose physical properties were reported at temperatures below 300 K [19]. The room temperature value of ρ is smaller than 5 mΩ cm and the κ is less than 1 W/mK [17,18,20]. The *ZT* of type-VIII BGS above room temperature was evaluated by using sintered samples whose carrier density was not fully optimized. Thereby, the maximum *ZT* of 0.2 was observed at 500 K [11,21].

* Corresponding author.
E-mail address: saiga@hiroshima-u.ac.jp (Y. Saiga).

0925-8388/$ – see front matter © 2010 Elsevier B.V. All rights reserved.
doi:10.1016/j.jallcom.2010.07.121

Table 1
Starting and crystal compositions of type-VIII $Ba_8Ga_{16}Sn_{30}$ crystals grown from Ga or Sn flux as determined by electron-probe microanalysis, lattice parameter a, and carrier density n.

Sample	Starting composition Ba:Ga:Sn	Crystal composition Ba:Ga:Sn	Lattice parameter a (Å)	Carrier density n (10^{19}/cm^3)
p-30	8:30:30	7.93:15.92:30.08	11.587 (3)	11
p-35	8:35:30	7.95:15.95:30.05	11.590 (2)	13
p-38	8:38:30	7.95:15.97:30.03	11.589 (2)	14
p-40	8:40:30	7.97:15.95:30.05	11.591 (2)	14
p-45	8:45:30	7.91:15.93:30.07	11.590 (3)	17
n-40	8:16:40	7.96:15.94:30.06	11.590 (3)	3.3
n-50	8:16:50	7.96:15.89:30.11	11.593 (2)	4.3
n-60	8:16:60	7.98:15.82:30.18	11.596 (2)	5.5

We have explored enhancing the ZT value of type-VIII BGS by tuning the carrier density. Furthermore, we have substituted Sb for Sn to increase the electron carrier density. The measurements of α, ρ, and κ and assessment of ZT at temperature between 300 K and 600 K are reported herein.

2. Experimental

Single crystals of type-VIII BGS were grown by the self-flux method, the details of which were described in previous papers [14,19,22]. The charge carrier type was tuned to be either p-type or n-type by using Ga or Sn flux [19]. The starting elements were placed in an evacuated quartz ampoule. The sample was heated up to 490 °C, and then slowly cooled to 390 °C, where the excess flux was removed in a centrifuge. The grown crystals were characterized by wave length dispersive electron-probe micro analysis (EPMA) by using a JEOL JXA-8200 analyzer. The crystal compositions were determined on the assumption that the total number of cage atoms in BGS is equal to 46. The compositions listed in Table 1 are averages over 5 regions of each crystal. While the amount of Sn in n-type samples increases by 0.01 with increasing the Sn flux amount, no increase of Ga content was observed in p-type samples within the resolution of EPMA even though the starting composition of Ga was increased from 30 to 45.

The single crystals were crushed into powder for the X-ray diffraction measurements. The diffraction patterns recorded with a Rigaku D/Tex Ultra detector indicated that all samples crystallize in the type-VIII clathrate structure. The lattice parameters determined by the Rietveld analysis are listed in Table 1. The lattice parameter for the n-type samples systematically increases with increasing Sn content. However, no systematic change is observed for the p-type samples within the experimental errors.

For the growth of Sb substituted crystals, we have chosen two sets of starting compositions Ba:Ga:Sn:Sb = 8:38:30:Y and 8:16:50:Y, where Y was increased up to 3.0 and 3.8, respectively, as shown in Table 2. The crystal composition and lattice parameter are also listed. The maximum amount of Sb in single crystals is approximately 0.8 irrespective of the used fluxes. It should be noted that the Ga composition increases from 16.0 to 16.8 with the increase of the Sb content from 0 to 0.83. Thus, the compositions of the single crystals are described as $Ba_8Ga_{16+x}Sn_{30-x-y}Sb_y$ ($x < 0.9$, $y < 0.9$). The charge balance would be maintained if x equals y. The lattice parameter decreases by 0.3% with the Sb substitution for both p- and n-type samples, being consistent with the smaller atomic volume of Sb than Sn.

Seebeck coefficient was measured using the MMR Measurement System in a vacuum at temperatures from 290 K to 600 K. Electrical resistivity was measured under the same condition with a dc four-probe method on a homemade system. For both measurements, we used same sample of 3 mm in length and 0.5 mm in thickness. The Hall coefficient R_H was measured at room temperature by a dc method in a magnetic field of 1 T. Carrier density n was determined from the relation $n = 1/eR_H$, where e is the electron charge. Thermal diffusivity D and specific heat C_p were simultaneously measured in a vacuum by the laser-flash method using a disk-shaped sample of 6 mm in diameter. The data of D and C_p were used to calculate thermal conductivity from the relationship $\kappa = DC_pd$, where d is the sample density.

Table 2
Starting and crystal compositions of type-VIII $Ba_8Ga_{16+x}Sn_{30-x-y}Sb_y$ crystals grown from Ga or Sn flux as determined by electron-probe microanalysis, and lattice parameter a.

Sample	Starting composition Ba:Ga:Sn:Sb	Crystal composition Ba:Ga:Sn:Sb	Lattice parameter a (Å)
p-38	8:38:30:–	7.95:15.97:30.03:–	11.589 (2)
p-Sb#1	8:38:30:1.5	8.01:16.41:29.04:0.55	11.598 (5)
p-Sb#2	8:38:30:1.5	8.00:16.67:28.61:0.72	11.575 (5)
p-Sb#3	8:38:30:3.0	8.02:16.81:28.36:0.83	11.563 (5)
n-50	8:16:50:–	7.96:15.89:30.11:–	11.593 (2)
n-Sb#1	8:16:50:2.5	8.01:16.57:28.62:0.81	11.573 (3)
n-Sb#2	8:16:50:3.8	7.96:16.25:29.37:0.38	11.586 (8)
n-Sb#3	8:16:50:2.5	8.02:16.34:29.15:0.51	11.569 (1)

3. Results and discussion

3.1. Thermoelectric properties of charge carrier-tuned $Ba_8Ga_{16}Sn_{30}$

Prior to presenting the temperature-dependent thermoelectric properties of the obtained crystals, we show in Fig. 1 the value of α at 300 K as a function of the excess flux amount. The values of α are positive and negative for the samples grown from Ga flux and Sn flux, respectively. In both cases, the absolute value $|\alpha|$ decreases monotonically with increasing the excess flux amount. This relation enables us to optimize the carrier density in both p-and n-type samples by tuning the excess flux amount.

For the samples p-38 and n-50, carrier densities n were estimated to be 1.4×10^{20} cm^{-3} and 4.3×10^{19} cm^{-3}, respectively, via $n = 1/eR_H$. By using a relation between α, n, and effective mass m^*, $\alpha = (8\pi^2 k_B^2 T/3eh^2)m^*(\pi/3n)^{2/3}$ relevant for degenerated semiconductors [23], the values of m^* were estimated to be $4.3m_e$ for p-38 and $1.5m_e$ for n-50, where m_e is the free electron mass. Furthermore, we calculated n for other samples by putting the value of α at 300 K in the above relation, thereby m^* was assumed to be equal among p-type samples and n-type samples, respectively.

As shown in Table 1, the Sn composition in the crystals systematically increases as the starting composition of Sn increases from 40 to 60. From the view point of the valence balance, excess Sn (Ga) composition from the ideal value of 30 (16) should give raise to electron (hole) carriers, which in turn decreases $|\alpha|$ as was

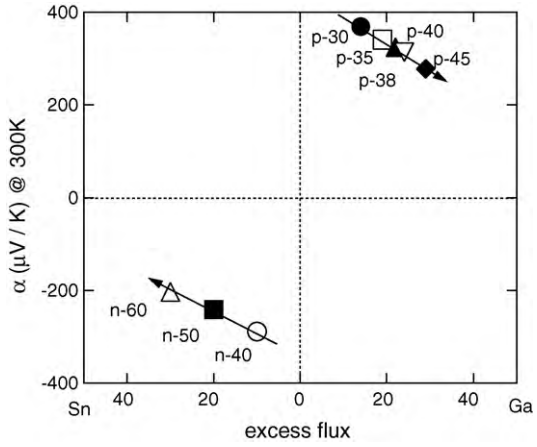

Fig. 1. Seebeck coefficient α at 300 K versus excess flux amounts for single crystals of $Ba_8Ga_{16}Sn_{30}$. The data for crystals grown from Sn and Ga fluxes are shown in the left and the right, respectively.

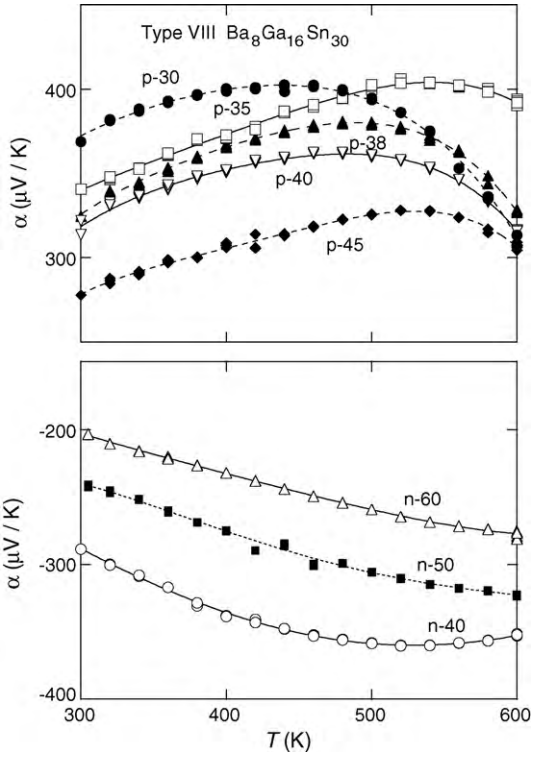

Fig. 2. Seebeck coefficient α as a function of temperature for type-VIII $Ba_8Ga_{16}Sn_{30}$ single crystals described in Table 1.

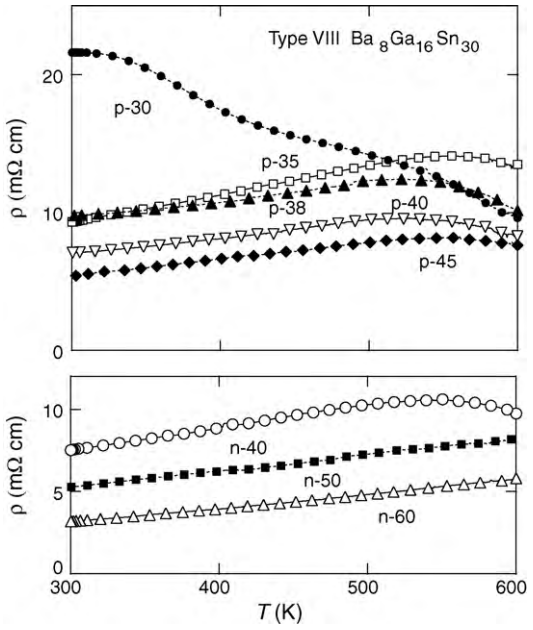

Fig. 3. Temperature dependence of electric resistivity ρ for type-VIII $Ba_8Ga_{16}Sn_{30}$ single crystals of p-type (upper) and n-type (lower).

observed. Nevertheless, the $|\alpha|$ even in heavily doped samples of p- and n-types maintains the value above 200 μV/K.

Fig. 2 shows the temperature dependences of α for p- and n-type samples. For p-type samples, $\alpha(T)$ has the maximum at around 500 K, which shifts to higher temperature along with the decrease in the maximal value in $\alpha(T)$. In analogy, a maximum in $|\alpha(T)|$ for n-50 and n-60 samples would appear at temperatures above 600 K. From these data of $\alpha(T)$ with the maximum at T_{max}, the thermal band gap E_g can be calculated according to the relation $E_g = 2\alpha_{max}T_{max}$ [9,10,24]. A mean value of $E_g = 0.37$ eV was obtained for the five p-type samples, and E_g of 0.38 eV was estimated for n-40 sample. These values of E_g agree with 0.32 eV obtained from a band structure calculation [25].

The data of $\rho(T)$ are presented in Fig. 3. For the sample p-30, ρ decreases from 22 mΩ cm with increasing temperature, being a characteristic of a doped semiconductor in the low-carrier region. For other p-type samples, ρ increases monotonically with increasing temperature and shows the maximum. The maximum temperature of 500–550 K for $\rho(T)$ is higher than that for $\alpha(T)$. The lowest values of $\rho(T = 300\,K)$ are 6 mΩ cm and 3 mΩ cm for the p- and n-type samples, respectively. For *n*-type samples, the decreasing trend in both $|\alpha|$ and ρ with the increase of Sn flux amount is consistent with the increase in the Sn composition of the crystals as shown in Table 1. Similar trend is observed in α and ρ for p-type samples, although no systematic increase in the Ga composition was detected by EPMA.

The temperature-dependent κ is shown in Fig. 4 for a selected sample n-50. For other samples, we could not obtain reliable data of κ because the crystal size was smaller than 6 mm, which diameter is required for the measurement by the laser-flash method. With increasing temperature, $\kappa(T)$ of n-50 shows a shallow minimum at around 450 K and gradually increases. This increase is connected with the excitation of minority p-type carriers over the band gap; bipolar thermal conduction [26]. The measured data were divided into lattice contribution κ_L and the electronic one κ_e on the assumptions as follows: (i) the bipolar thermal conduction κ_b contributes to κ_e only above 400 K, (ii) below 400 K, κ_L is equal to the difference $\kappa - \kappa_{WF}$ where $\kappa_{WF} = LT/\rho$ with $L = 2.44 \times 10^{-8}$ WΩ/K^2, (iii) κ_L becomes constant above 400 K. Then, κ_e was calculated from relation $\kappa_e = \kappa - \kappa_L$. Thus estimated value of $\kappa_L(T)$ for n-50 is presented by the broken line in Fig. 4. In order to estimate the values of $\kappa(T)$ for other samples, we assumed that κ_L and κ_b do not depend on samples. This crude assumption may be allowed because the variations in $|\alpha|$ and ρ are not so strong among the measured samples with n- and p-type carriers, respectively. Then, $\kappa(T)$ for each sample can be calculated as $LT/\rho + \kappa_L$ (n-50) + κ_b (n-50).

Fig. 5 shows the *ZT* calculated from α, ρ and κ for all BGS single crystals. Among p-type samples, the lowest *ZT* value is observed in the sample p-30 showing the semiconducting resistivity. The sample p-40 has the highest *ZT* value with the maximum of 1.0 at around 450 K. Because the *ZT* value of p-45 is lower than p-40, the carrier density might be optimized in p-40 among p-type samples. By contrast, all the n-type sample n-40, n-50, and n-60 have com-

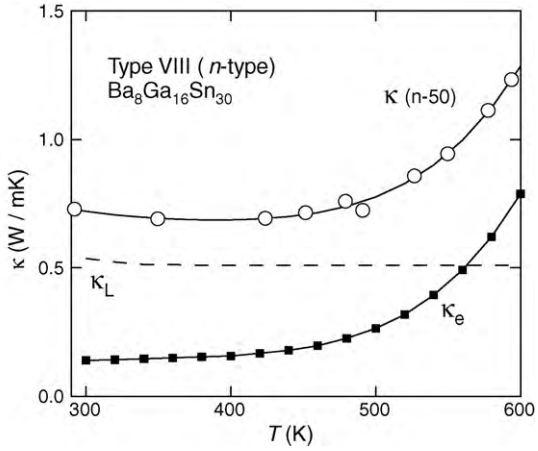

Fig. 4. Temperature dependences of total thermal conductivity κ, electronic thermal conductivity κ_e, and the lattice thermal conductivity κ_L for type-VIII $Ba_8Ga_{16}Sn_{30}$ (n-50).

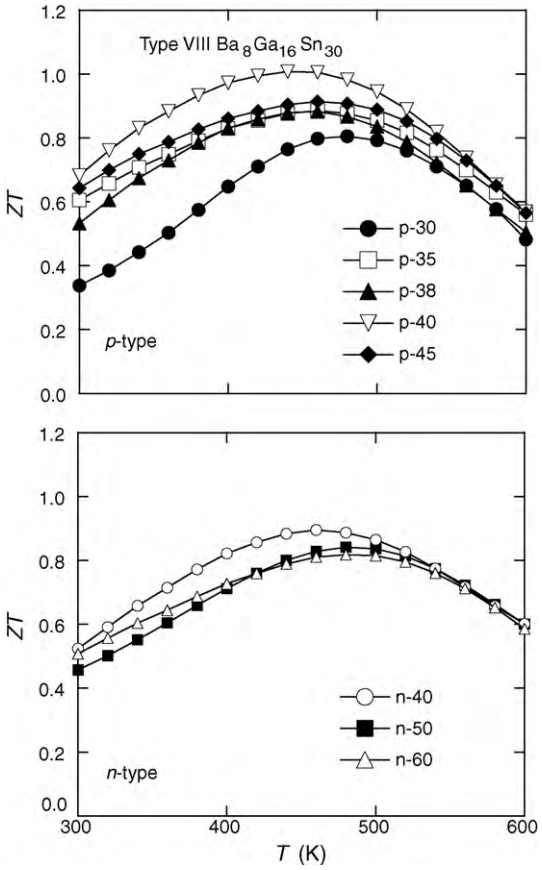

Fig. 5. Temperature dependences of the dimensionless figure of merit *ZT* values for p-type (upper) and n-type (lower) samples of type-VIII $Ba_8Ga_{16}Sn_{30}$.

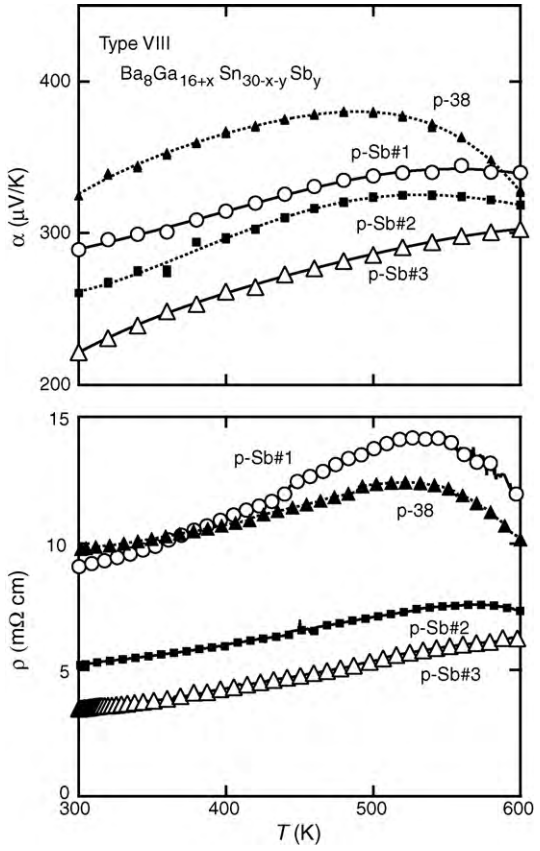

Fig. 6. Seebeck coefficient α (upper) and electrical resistivity ρ (lower) as a function of temperature for type-VIII $Ba_8Ga_{16+x}Sn_{30-x-y}Sb_y$ and $Ba_8Ga_{16}Sn_{30}$ (p-38).

parable *ZT* values in the whole temperature range. The maximum of *ZT* = 0.9 appears for n-40 at 450 K.

3.2. Thermoelectric properties of $Ba_8Ga_{16+x}Sn_{30-x-y}Sb_y$

The single crystals of $Ba_8Ga_{16+x}Sn_{30-x-y}Sb_y$ (BGSS) were characterized by EPMA and X-ray diffraction analysis as well as measurements of $\alpha(T)$ and $\rho(T)$. All the specimens cut from crystals grown from Ga flux (initial composition = 38) had positive α. However, the specimens cut from crystals grown from Sn flux (initial composition = 50) displayed either negative or positive values of α. This means the presence of inhomogeneity in the composition in the crystals grown from Sn flux, although corresponding deviation of the composition was not detected by our EMPA. Therefore, we report here the thermoelectric properties only for the p-type samples.

Fig. 6 displays α and ρ as a function of temperature for the p-type samples of BGSS. Both α and ρ at 300 K decrease with the increase of Sb amount *y* from 0 in p-38 to 0.83 in p-Sb#3. In the whole temperature range, $\rho(T)$ of p-Sb#3 is still lower than that of p-45 exhibiting the lowest $\rho(T)$ among the non Sb-doped samples (see Fig. 3). Thus, it is proved that Sb substitution for Sn in BGS creates p-type carriers, as opposite to our initial expectation for electron doping.

The *ZT* values for the BGSS samples are shown in Fig. 7 as a function of temperature. For the calculation of *ZT*, we used the κ value estimated from the sum of κ_L(n-50) + κ_b(n-50) + LT/ρ. Compared with *ZT* for the reference sample of p-38, the *ZT* values for p-Sb#2 and p-Sb#3 are enhanced. Especially, the maximum for p-Sb#2 reaches 0.98 at around 480 K.

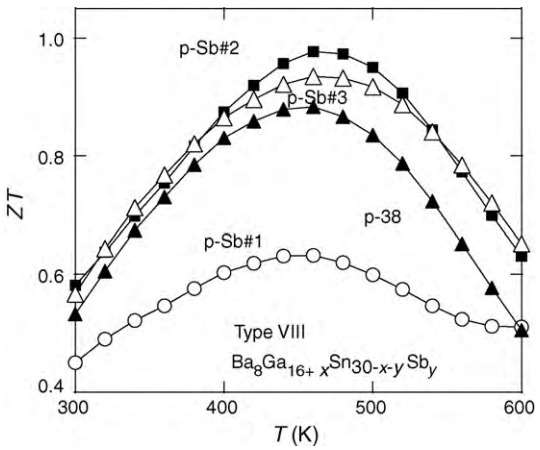

Fig. 7. *ZT* values as a function of temperature for p-type samples of type-VIII $Ba_8Ga_{16+x}Sn_{30-x-y}Sb_y$.

4. Summary and conclusion

In order to maximize the *ZT* value in p- and n-type samples of type-VIII $Ba_8Ga_{16}Sn_{30}$, we have tuned the charge carrier density by two methods. First, in the crystal growth by the self-flux method, the initial compositions of Ga and Sn were varied in the ranges 30–45 for Ga and 40–60 for Sn. It is found that the increase in the initial amounts of Ga and Sn results in doping of p-type and n-type carriers, respectively. In fact, the carrier density increases from $1.1 \times 10^{20}/cm^3$ to $1.7 \times 10^{20}/cm^3$ in p-type samples and from $3.3 \times 10^{19}/cm^3$ to $5.5 \times 10^{19}/cm^3$ in n-type samples. Thus optimized samples with p- and n-type carriers have *ZT* values of 1.0

and 0.9, respectively, in the temperature range between 450 K and 500 K. Partial substitution of Sb for Sn was used as another method to tune the charge carrier density. With the increase of the Sb content in the crystal, the Ga content was found to be increased. Thus, the crystal composition is described as $Ba_8Ga_{16+x}Sn_{30-x-y}Sb_y$ ($x < 0.9$, $y < 0.9$). The highest ZT for the BGSS with p-type carriers was 1.0 at 480 K. Consequently, type-VIII BGS clathrates with optimized carriers of both p- and n-types are promising materials for thermoelectric converters to recover waste heat at temperatures 400–600 K.

Acknowledgments

We thank Y. Shibata for the EPMA performed at Natural Science Center for Basic Research and Development, Hiroshima University. We are grateful to T. Takeuchi for the generous use of MMR Measurement System for the measurement of Seebeck coefficient. This work was supported by a NEDO, grant no. 09002139-0 and Grant-in-Aid for Scientific Research from MEXT of Japan, grants no. 1824032, no. 19051011, and no. 20102004.

References

[1] D.M. Rowe (Ed.), Thermoelectrics Handbook: Macro to Nano, CRC Press, Taylor & Francies Group, Boca Raton, 2006.
[2] G.S. Nolas, J. Sharp, H.J. Goldsmid, Thermoelectrics: Basic Principles New Materials Developments, Springer, New York, 2001.
[3] K.F. Hsu, S. Loo, F. Guo, W. Chen, J.S. Dyck, C. Uher, T. Hogan, E.K. Polychroniadis, M.G. Kanatzidis, Science 303 (2004) 818.
[4] G. Nakamoto, K. Kinoshita, M. Kurisu, J. Alloys Compd. 436 (2007) 65.
[5] K.A. Kovnir, A.V. Shevelkov, Russ. Chem. Rev. 73 (2004) 923.
[6] P. Rogl, in: D.M. Rowe (Ed.), Thermoelectrics Handbook: Macro to Nano, CRC, Boca Raton, 2006, p. 32.
[7] E.S. Toberer, A.F. May, G.J. Snyder, Chem. Mater. 22 (2010) 624.
[8] M. Christensen, S. Johnsen, B.B. Iversen, Dalton Trans. 39 (2010) 978.
[9] A.F. May, E.S. Toberer, A. Saramat, G.J. Snyder, Phys. Rev. B 80 (2009) 125205.
[10] D. Cederkrantz, A. Saramat, G.J. Snyder, A.E.C. Palmqvist, J. Appl. Phys. 106 (2009) 074509.
[11] V.L. Kuznetsov, L.A. Kuznetsova, A.E. Kaliazin, D.M. Rowe, J. Appl. Phys. 87 (2000) 7871.
[12] I. Fujita, K. Kishimoto, M. Sato, H. Anno, T. Koyanagi, J. Appl. Phys. 99 (2006) 093707.
[13] G.A. Slack, in: D.M. Rowe (Ed.), CRC handbook of Thermoelectrics, CRC, Boca Raton, 1995, p. 407.
[14] D. Huo, T. Sakata, M.A. Avila, M. Tsubota, F. Iga, H. Fukuoka, S. Yamanaka, S. Aoyagi, T. Takabatake, Phys. Rev. B 71 (2005) 075113.
[15] W.C. Cabrera, R.C. Gil, V.H. Tran, Y. Grin, Z. Kristallogr, New Cryst. Struct. 217 (2002) 181.
[16] G.S. Nolas, J.L. Cohn, J.S. Dysk, C. Uher, G.A. Lamberton, T.M. Tritt, J. Mater. Res. 19 (2004) 3556.
[17] M.A. Avila, K. Suekuni, K. Umeo, H. Fukuoka, S. Yamanaka, T. Takabatake, Appl. Phys. Lett. 92 (2008) 041901.
[18] K. Suekuni, M.A. Avila, K. Umeo, H. Fukuoka, S. Yamanaka, T. Nakagawa, T. Takabatake, Phys. Rev. B 77 (2008) 235119.
[19] M.A. Avila, D. Huo, T. Sakata, K. Suekuni, T. Takabatake, J. Phys.: Condens. Matter 18 (2006) 1585.
[20] M.A. Avila, K. Suekuni, K. Umeo, H. Fukuoka, S. Yamanaka, T. Takabatake, Phys. Rev. B 74 (2006) 125109.
[21] M. Hayashi, K. Kishimoto, K. Kishio, K. Akai, H. Asada, T. Koyanagi, Dalton Trans. 39 (2010) 1113.
[22] M.A. Avila, K. Suekuni, K. Umeo, T. Takabatake, Physica B 383 (2006) 124.
[23] G.J. Snyder, E.S. Toberer, Nat. Mater. 7 (2008) 105.
[24] H.J. Goldsmid, J.W. Sharp, J. Electron. Mater. 28 (1999) 869.
[25] Y. Kono, N. Ohya, T. Taguchi, M.A. Avila, K. Suekuni, T. Takabatake, S. Yamamoto, K. Akai, J. Appl. Phys. 107 (2010) 123720.
[26] H.J. Goldsmid, Introduction to Thermoelectricity, Springer, Heidelberg, 2010.